A statistical shape model to predict the premorbid glenoid cavity

Daniel Abler[1], PhD, Steve Berger[1], PhD, Alexandre Terrier[2], PhD Fabio Becce[3], MD, Alain Farron[4], MD & Philippe Büchler[1], PhD

[1]Institute for Surgical Technology and Biomechanics, University of Bern, Bern, Switzerland [2]Laboratory of Biomechanical Orthopedics, Ecole Polytechnique Fédérale de Lausanne, Lausanne, Switzerland;[3]Department of Diagnostic and Interventional Radiology, Lausanne University Hospital, Lausanne, Switzerland; [4]Service of Orthopedics and Traumatology, Lausanne University Hospital, Lausanne, Switzerland

Contributor responsible for the manuscript and proofs:

Prof. Dr. Philippe Büchler

Institute for Surgical Technology and Biomechanics, University of Bern, Stauffacherstrasse 78, CH- 3014 Bern, Switzerland

philippe.buechler@istb.unibe.ch

Disclaimer: No outside funding or grants was received for this study.

IRB: Commission cantonale d'éthique (CER-VD)**,** Protocol 136/15

Short title: Glenoid prediction using statistical shape modeling

Total word count: 3162

Abstract

Background: This study proposes a method for inferring the premorbid glenoid shape and orientation to inform restorative surgery.

Methods: We developed a statistical shape model (SSM) from 64 healthy scapulae. The premorbid glenoid shape was predicted from the surrounding scapular body using a SSM-based reconstruction method. First, the method was validated on 64 healthy scapulae by quantifying the accuracy of the predicted surface in terms of surface distance, as well as glenoid version and inclination. The SSM-based reconstruction was then applied to 30 scapulae with OA glenoids. Glenoid version and inclination were measured fully automatically and compared between the original OA glenoids, SSM-based glenoid reconstructions, and healthy scapulae.

Results: Validation on healthy scapulae showed a root mean square surface distance between original and predicted glenoid cavities of 1.0mm±0.2mm. The prediction error was 2.1°±1.6° for glenoid version and 2.1°±1.8° for inclination. Differences between original and predicted glenoid measurements were not statistically significant ($p \geq 0.42$). When applied to OA dataset, SSM-based reconstruction restored the glenoid version and inclination to values similar to the healthy situation. No differences were observed between SSM-based reconstructed glenoids and healthy scapulae ($p \geq 0.44$), while reconstructed glenoids significantly differed from original scapulae with OA glenoids ($p \leq 0.03$).

Conclusion: The proposed local SSM can accurately predict the premorbid glenoid cavity of healthy scapulae from anatomic features regarded as unaffected by degeneration. This technique

has the potential to reconstruct the premorbid glenoid cavity as it was prior to OA, and thus guide the orientation of glenoid implants in total shoulder arthroplasty.

Level of evidence: Basic Science Study; Computer Modeling

Keywords: Glenoid, Total Shoulder Arthroplasty, Computed Tomography, 3D Reconstruction, Statistical Shape Model, Version, Inclination

Introduction

Patients suffering from shoulder osteoarthritis (OA) may exhibit severe wear of their glenohumeral joint[9] and various deformity patterns of the glenoid cavity[1,10,17]. When nonsurgical treatments fail, shoulder arthroplasty can be performed to replace the degenerated glenohumeral joint by prostheses. Accurate positioning of the glenoid component is crucial for the long-term success of total shoulder arthroplasty[15] as incorrect positioning can lead to glenoid implant failure and/or glenohumeral subluxation and/or dislocation[5,7]. When glenohumeral OA is unilateral, the patient-specific orientation of the glenoid implant might be determined based on the healthy contralateral shoulder. However, glenohumeral OA is often bilateral so that the original orientation, size, and shape of the glenoid cavity is usually unknown at the time of surgery.

Different techniques have been proposed to correct pathologic glenoid version due to OA[6,25]. One of these approaches relied on positioning a three-dimensional reference model of the glenoid vault on the endosteal surface of the pathologic bone[25]. More recently, this method has been compared to predictions of the glenoid orientation based on landmarks located on the body of the scapula. A linear relation was found between the anterior glenoid wall angle – defined by these landmarks – and the glenoid version of healthy scapulae[6]. These previous studies indicate that a correlation exists between healthy glenoid anatomy and the morphology of structures unaffected by OA, which may allow predicting healthy glenoid version. However, such correlation alone provides no information about the glenoid's three-dimensional shape or orientation.

Statistical shape modeling (SSM) is a method that identifies the average and principal variations of shape within a training population. One strength of this method is its ability to extrapolate a complete anatomic surface representation from a sparse set of spatial positions. For example, SSM has been used previously to predict the complete shape of the human femur from a sparse set of landmarks collected on its proximal surface[24] or to predict the premorbid shape of the proximal humerus[23]. Recently, SSM has also been proposed for the reconstruction of glenoid bone defects[22]. While the authors showed that this approach accurately reconstructs the shape of healthy scapulae, they did not evaluate the performance of this method on scapulae affected by OA.

Similar to this recent study[22], we have developed an SSM-based approach for reconstructing the "healthy" surface of glenoid cavities affected by OA. Instead an SSM of the entire scapula, we propose using a local SSM, centered around the glenoid bone. Our first objective was to quantify the accuracy of SSM-based predictions on a population with no signs of scapula deformation by comparing the glenoid cavity predicted by the SSM to the actual three-dimensional glenoid anatomy. The second objective of this work was to evaluate the ability of the SSM model to predict the premorbid glenoid cavity and its orientation for patients exhibiting different patterns of glenohumeral OA.

Materials & Methods

Our study was performed in three main steps. First, a 'local' SSM was created from a dataset of healthy scapulae (i.e. with no signs of pathology on computed tomography (CT)), which was used to reconstruct glenoid shape based solely on information from the bony regions surrounding it (Fig. 1). In a second step, the SSM-based prediction method was tested on healthy scapulae for validation. Finally, the method was used to predict the premorbid shape of scapulae with glenoids affected by OA.

Statistical Shape Model

A dataset of 64 healthy scapulae (42 men, 22 women, between 17 and 88 years of age, average age of 59.6 years) was used in this IRB-approved study (protocol 136/15). Consecutive whole-body CT scans (64-detector row CT system) of polytrauma patients were retrospectively reviewed by an experienced musculoskeletal radiologist. Patients with CT signs of glenohumeral OA, glenoid dysplasia, scapular fracture, previous shoulder surgery, motion or any other CT artifacts, and incomplete coverage of the scapulae were excluded. CT images of these scapulae were subsequently segmented manually, and models of their 3D shape were generated as surface meshes. Models of left scapulae were mirrored to resemble the configuration of right scapulae. The positions of all corresponding anatomic landmarks were established automatically for all the bones in the dataset[18,19]. With this information, the average healthy scapula shape and its modes of variations could be computed[14], defining the SSM and describing how anatomic landmarks

move together when the shape of the scapula changes (Fig. 2). This study used a 'local' SSM that did not include the entire scapula, but only the region of the glenoid as shown in Figure 1.

Validation on Healthy Scapulae

The shape of the healthy glenoid was reconstructed by fitting the SSM to the scapula region surrounding the glenoid on the target shape (Fig. 1). The fitting was performed by adjusting the contribution of each mode of variation of the SSM until the predicted shape best matched the shape of the target bone in the region for fitting (Fig. 1, red surface). The SSM describes how the proportions of different parts of the shape are linked. Therefore, the parameter set that optimally fits the bone surrounding the glenoid also simultaneously provides a prediction of the glenoid cavity. Since the SSM was built from healthy scapulae, the predicted glenoid cavity has the characteristics of a healthy or premorbid glenoid. Thus, this approach provides an approximation of healthy glenoid shape for the particular scapula used as fitting target.

The SSM creation and prediction process was repeated for each of the 64 scapulae in a leave-one-out analysis. In each repetition, one scapula was selected and the SSM was built from the remaining 63 scapulae. This SSM was then used to predict the overall surface of the scapula that had been "left out" from the SSM creation process (Fig. 1).

A semi-automated CT measurement method was adapted and fully automatized to quantify glenoid version, inclination, and medialization in a standardized and reproducible way[27]. The original semi-automated method uses 11 bony landmarks that are placed manually on the non-eroded

scapula to define a coordinate system in relation to which glenoid characteristics can be quantified. Our fully automatized approach leverages the SSM to transfer the positions of these landmarks automatically from the surface model of a single scapula to the surface models of all individual scapula[21]. As the resulting landmark positioning tends to be slightly inaccurate in practice, the positions of the landmarks were automatically corrected based on the local curvature of the scapula, following the same criteria as for manual landmark placement.[27] The resulting scapula coordinate system was then used to quantify glenoid version, inclination, and medialization.

Accuracy of predictions was evaluated in each repetition of the leave-one-out analysis. The quality of shape prediction was quantified using the distance between the reconstructed glenoid cavity and the surface of the bone obtained from its segmentation. We report the root mean square (RMS) distance error for the glenoid cavity and the entire predicted shape, which includes the bony regions used for the fitting process. The difference between measurements of the original and reconstructed glenoids was evaluated using Bland-Altman plots. Statistical significance ($p<0.05$) was checked with paired Student's t-tests. Average cohort results were reported as mean ± standard deviation of absolute (unsigned) difference between original and reconstructed measures.

Premorbid Shape of OA Glenoids

Preoperative nonarthrographic shoulder CT scans of 30 patients who underwent anatomic total shoulder arthroplasty for primary glenohumeral OA were randomly selected from our institutional database (18 men, 12 women, between 54 and 88 years of age, average age of 71 years). Patterns of glenoid OA were classified according to the updated Walch grading system[1] by the same

musculoskeletal radiologist, in consensus with an experienced shoulder surgeon (Table I). The scapulae were manually segmented, and models of their 3D shape were generated as surface meshes.

Prediction of the premorbid shape followed the same procedure as for the validation study on healthy scapulae. Glenoid version, inclination, and medialization were quantified by the fully automatized measurement method described previously. Differences in these measurements between the original scapulae with OA and the reconstructed premorbid shapes were statistically evaluated using paired Student's t-tests; differences to healthy glenoids were assessed using two sample Student's t-tests. The significance level set was at $p<0.05$.

Results

Statistical Shape Model

The SSM was built from all healthy scapulae of the training dataset. The first 3 modes of variation represented more than 60% of the overall shape variability across subjects (Fig. 2), while less than 20 modes of the SSM explained about 95% of shape variability. Although the modes of variation do not have direct morphologic interpretation, the first few modes of the scapula SSM displayed characteristic features: the first mode of variation was associated with a change in size, the second mode predominantly reflected a change in angle between the acromion and the coracoid, while the third mode was related to variations in glenoid inclination (Fig. 2).

Validation on Healthy Scapulae

The leave-one-out analysis for evaluating glenoid reconstruction accuracy showed that the SSM accurately reproduces the surface of the glenoid region (Fig. 3). On average, the RMS reconstruction error was slightly above 0.5mm on the bone surface used for fitting (0.6mm±0.1mm). The reconstruction error was larger for the predicted glenoid cavity, yet its average error remained at 1mm (1.0mm±0.2mm). Figure 3 shows the spatial distribution of surface distance between original and SSM-based reconstructed glenoids. Surface distance of the subjects with the smallest (Fig. 3b) and largest (Fig. 3c) reconstruction error on the glenoid cavity were compared to the average surface distance across all samples (Fig. 3a). Surface distance remained below 1mm on most of the reconstructed surface, yet could reach up to approximately 3.5mm on the superior aspect of the glenoid rim in the worst fitting sample.

Heathy scapulae included in this study had a glenoid version of 8.1°±5.2°, inclination of 8.6°±5.3°, and medialization of 19.2mm±1.8 mm. The average absolute difference between AAM-based reconstructed and the healthy reference glenoids was 2.1°±1.6° for glenoid version, 2.1°±1.8° for inclination, and 0.7mm±0.5mm for medialization, with 95% confidence intervals between -5.2° and 5.3° for glenoid version, -5.5° and 5.4° for inclination, and -1.7 mm and 1.8 mm for medialization (Fig. 4). The prediction error was almost independent of the magnitude of the respective measurements. No significant differences were found between the glenoid version ($p=0.93$), inclination ($p=0.97$), and medialization ($p=0.42$) of the SSM-based reconstructed and healthy reference glenoids.

Premorbid Shape of OA Glenoids

The shape of the premorbid glenoid was reconstructed for each of the 30 OA samples. Overall, the SSM-based reconstruction restored glenoid orientation with values of version and inclination close to the healthy situation (Fig. 5). Statistical analysis revealed no difference between SSM-based reconstructed glenoid version and the healthy situation ($p=0.97$), whereas the version of the original OA glenoids was significantly different from the version of the SSM-based reconstructed glenoids ($p<0.01$) and of the healthy situation ($p<0.01$). Similar results were obtained for the glenoid inclination, where no difference was observed between SSM-based reconstructed and healthy configurations ($p=0.44$), while the inclination of the original OA glenoids was significantly different from both the SSM-based reconstructed ($p=0.03$) and healthy ($p=0.02$) scapulae (Fig. 5). On the other hand, medialization was not significantly influenced by the SSM-based reconstruction.

Our OA dataset included samples of six different Walch classes (Table I). The model was able to correct the posterior version for the B3, B2, and A2 OA glenoid types, with the largest correction for B3 and lowest for A2 glenoids. On the other hand, the correction for the A1 and B1 glenoid types was close to zero. SSM-based reconstruction increased the inclination for all Walch classes, except for type D where a decrease of approximately 4° was measured. Again, the medialization was not affected by the reconstruction and remained constant.

Discussion

Optimal glenoid implant positioning is challenging for patients suffering from glenohumeral OA with substantial wear of the glenoid cavity. This study shows that an approach based on SSM provides an accurate prediction of the entire three-dimensional surface of the healthy glenoid and is able to reconstruct the premorbid glenoid orientation of pathologic scapulae.

Validation of the SSM-based technique on healthy scapulae indicates that the premorbid shape can be reconstructed with millimeter accuracy. Our results (1.0mm RMS error) are similar to the data recently reported by Plessers et al.[22] using a SSM of the entire scapula shape (1.2mm RMS error). Since clinical shoulder CT scans have a spatial resolution of the same magnitude, this level of prediction accuracy is comparable with the accuracy by which a glenoid could be reconstructed in 3D from an actual CT dataset. The validation on healthy cases also showed that the glenoid version can be predicted with an error around 2°, which is comparable to the results obtained by Plessers et al.[22] using a SSM of the scapula (2.9°), but smaller than the prediction error of the glenoid vault model proposed by Scalise et al.[25] (3.7°) and the anterior glenoid wall angle model developed by Ganapathi et al.[6] (3.2°). Overall, the precision by which the SSM model reproduced the healthy glenoid orientation is of the same magnitude as the precision of glenoid implant positioning using patient-specific guides, which has been reported between 1.8° and 4.3° for version and between 1.2° and 3.1° for inclination[4,8,11,12].

Clinical applicability of the SSM-based glenoid reconstruction approach was demonstrated on scapulae with various OA glenoid patterns. Prediction results of glenoid version and inclination

followed the clinical intuition for each Walch class, applying a larger correction on the version where the wear was larger and leaving the version unchanged otherwise. Statistically, predicted glenoid version and inclination were compatible with characteristics of a healthy scapula dataset, but significantly different from the original OA shapes. This evaluation on scapulae with OA glenoids demonstrates that the proposed reconstruction process restores glenoid orientation.

Validation of the prediction accuracy on individual scapulae remains challenging as it requires knowledge of the shape of the scapula prior to degradation by OA. Cases of unilateral glenohumeral OA deformation provide a route for validating such studies; however, these are relatively rare and difficult to obtain from routine CT data. Furthermore, it remains unclear if the non-OA side is truly normal and if these patients had symmetric scapulae before pathologic deformation[26]. Therefore, a longitudinal dataset of shoulder CT scans would be needed, which follows patients from the premorbid state to fully developed glenohumeral OA, eventually requiring shoulder arthroplasty. Despite the difficulties to fully validate the proposed procedure for reconstructing OA glenoids in individual patients, SSM-based prediction of shoulder anatomy could also be used in various other clinical settings. For example, in cases of bony Bankart fractures, the method could support the surgical decision-making process by pre-surgical reconstruction of the premorbid glenoid position and orientation.

The measurement of glenoid version is traditionally based on a 2D approach using a specific axial CT slice. This approach has been shown to be inaccurate as it depends on the position of the scapula – and thus of the patient – as visualized on the CT slice, and does not account for bone

erosions outside of the axial CT plane[2,3,9,20]. Several methods have been developed to take into account the three-dimensional nature of the scapula anatomy[6,13,16], yet their implementation in clinical practice remains challenging and they are limited to a few anatomic measurements. On the other hand, the SSM-based approach proposed here, not only predicts these clinical measurements, but also the entire shape of the original glenoid cavity. Since the error of the surface reconstruction is small, we believe that glenoid implant positioning based on the complete 3D shape will be more robust and thus represents a better predictor for preoperative planning.

A preliminary analysis had shown that the prediction of the glenoid cavity was more accurate when the SSM only included the glenoid, parts of the acromion and coracoid, instead of the entire scapula. An additional advantage of this approach is that the tips of the acromion and coracoid can be excluded from the model. These regions are difficult to segment from CT images and not always fully included in the original CT field of view for radiation protection reasons. By excluding these regions, we obtained improved prediction accuracy of healthy scapulae, while removing error-prone surface information from the fitting process.

This study has limitations. First, the number of samples in each Walch class does not permit conclusions about statistical significance by subgroup. However, the orientation correction observed for each Walch class agrees with clinical intuition. Moreover, this technique allowed restoring average version and inclination of glenoids affected by a representative range of OA-induced deformations to values characteristic for the healthy population. A further limitation concerns the size of the glenoid region that is expected to be affected by OA and therefore excluded

from the fitting process (Fig. 1). We assumed that the osteoarthritic deformation was limited to the area in close proximity to the glenoid cavity, but OA might affect other regions and extend to the acromion and coracoid. Our results indicate that the proposed approach is suitable for correcting OA-induced glenoid deformations, yet for future clinical application, SSM-based predictions should be further evaluated.

Conclusions

This study shows that it is possible to rely on a local SSM to predict the three-dimensional shape of the glenoid cavity with an average surface reconstruction error of 1 mm, and the glenoid orientation with a precision of approximately 2°. Moreover, glenoid version and inclination reconstructed from OA datasets are statistically comparable with healthy scapulae. This approach provides a quantitative method to help clinicians in preoperatively determining the glenoid implant orientation in patients with glenohumeral OA.

References

1. Bercik MJ, Kruse K, Yalizis M, Gauci M-O, Chaoui J, Walch G. A modification to the Walch classification of the glenoid in primary glenohumeral osteoarthritis using three-dimensional imaging. J. Shoulder Elbow Surg. [Internet]. 2016 Jun 6;Available from: http://www.ncbi.nlm.nih.gov/pubmed/27282738doi:10.1016/j.jse.2016.03.010

2. Bokor DJ, O'Sullivan MD, Hazan GJ. Variability of measurement of glenoid version on computed tomography scan. J. shoulder Elb. Surg. [Internet]. 1999 Nov;8(6):595–8. Available from: http://www.ncbi.nlm.nih.gov/pubmed/10633895doi:10.1016/S1058-2746(99)90096-4

3. Budge MD, Lewis GS, Schaefer E, Coquia S, Flemming DJ, Armstrong AD. Comparison of standard two-dimensional and three-dimensional corrected glenoid version measurements. J. shoulder Elb. Surg. [Internet]. 2011 Jun;20(4):577–83. Available from: http://www.ncbi.nlm.nih.gov/pubmed/21324716doi:10.1016/j.jse.2010.11.003

4. Eraly K, Stoffelen D, Vander Sloten J, Jonkers I, Debeer P. A patient-specific guide for optimizing custom-made glenoid implantation in cases of severe glenoid defects: An in vitro study. J. Shoulder Elb. Surg. [Internet]. 2016;25(5):837–845. Available from: http://dx.doi.org/10.1016/j.jse.2015.09.034doi:10.1016/j.jse.2015.09.034

5. Farron A, Terrier A, Büchler P. Risks of loosening of a prosthetic glenoid implanted in

retroversion. J. shoulder Elb. Surg. [Internet]. 2006 Jul;15(4):521–6. Available from: http://www.ncbi.nlm.nih.gov/pubmed/16831661doi:10.1016/j.jse.2005.10.003

6. Ganapathi A, McCarron JA, Chen X, Iannotti JP. Predicting normal glenoid version from the pathologic scapula: A comparison of 4 methods in 2- and 3-dimensional models. J. Shoulder Elb. Surg. [Internet]. 2011;20(2):234–244. Available from: http://dx.doi.org/10.1016/j.jse.2010.05.024doi:10.1016/j.jse.2010.05.024

7. Hasan SS, Leith JM, Campbell B, Kapil R, Smith KL, Matsen FA. Characteristics of unsatisfactory shoulder arthroplasties. J. shoulder Elb. Surg. [Internet]. 2002 Sep;11(5):431–41. Available from: http://www.ncbi.nlm.nih.gov/pubmed/12378161doi:10.1067/mse.2002.125806

8. Hendel MD, Bryan JA, Barsoum WK, Rodriguez EJ, Brems JJ, Evans PJ, et al. Comparison of Patient-Specific Instruments with Standard Surgical Instruments in Determining Glenoid Component Position. J. Bone Jt. Surgery-American Vol. [Internet]. 2012;94(23):2167–2175. Available from: http://content.wkhealth.com/linkback/openurl?sid=WKPTLP:landingpage&an=00004623-201212050-00010doi:10.2106/JBJS.K.01209

9. Hoenecke HR, Hermida JC, Flores-Hernandez C, D'Lima DD. Accuracy of CT-based measurements of glenoid version for total shoulder arthroplasty. J. shoulder Elb. Surg. [Internet]. 2010 Mar;19(2):166–71. Available from:

http://www.ncbi.nlm.nih.gov/pubmed/19959378doi:10.1016/j.jse.2009.08.009

10. Iannotti JP, Jun B-J, Patterson TE, Ricchetti ET. Quantitative Measurement of Osseous Pathology in Advanced Glenohumeral Osteoarthritis. J. Bone Jt. Surg. [Internet]. 2017;99(17):1460–1468. Available from: http://insights.ovid.com/crossref?an=00004623-201709060-00006doi:10.2106/JBJS.16.00869

11. Iannotti JP, Weiner S, Rodriguez E, Subhas N, Patterson TE, Jun BJ, et al. Three-Dimensional Imaging and Templating Improve Glenoid Implant Positioning. J. Bone Jt. Surgery-American Vol. [Internet]. 2015;97(8):651–658. Available from: http://content.wkhealth.com/linkback/openurl?sid=WKPTLP:landingpage&an=00004623-201504150-00006doi:10.2106/JBJS.N.00493

12. Levy JC, Everding NG, Frankle MA, Keppler LJ. Accuracy of patient-specific guided glenoid baseplate positioning for reverse shoulder arthroplasty. J. Shoulder Elb. Surg. [Internet]. 2014;23(10):1563–1567. Available from: http://dx.doi.org/10.1016/j.jse.2014.01.051doi:10.1016/j.jse.2014.01.051

13. Lewis GS, Armstrong AD. Glenoid spherical orientation and version. J. shoulder Elb. Surg. [Internet]. 2011 Jan;20(1):3–11. Available from: http://www.ncbi.nlm.nih.gov/pubmed/20932782doi:10.1016/j.jse.2010.05.012

14. Lüthi M, Blanc R, Albrecht T, Gass T, Goksel O, Büchler P, et al. Statismo-A framework

for PCA based statistical models. Insight J. 2012;1:1–18.

15. Matsen FA, Clinton J, Lynch J, Bertelsen A, Richardson ML. Glenoid component failure in total shoulder arthroplasty. J. Bone Joint Surg. Am. [Internet]. 2008 Apr;90(4):885–96. Available from: http://www.ncbi.nlm.nih.gov/pubmed/18381328doi:10.2106/JBJS.G.01263

16. Moineau G, Levigne C, Boileau P, Young A, Walch G, French Society for Shoulder & Elbow (SOFEC). Three-dimensional measurement method of arthritic glenoid cavity morphology: feasibility and reproducibility. Orthop. Traumatol. Surg. Res. [Internet]. 2012 Oct;98(6 Suppl):S139-45. Available from: http://www.ncbi.nlm.nih.gov/pubmed/22964089doi:10.1016/j.otsr.2012.06.007

17. Mullaji AB, Beddow FH, Lamb GH. CT measurement of glenoid erosion in arthritis. J. Bone Joint Surg. Br. [Internet]. 1994 May;76(3):384–8. Available from: http://www.ncbi.nlm.nih.gov/pubmed/8175838

18. Mutsvangwa T, Burdin V, Schwartz C, Roux C. An automated statistical shape model developmental pipeline: application to the human scapula and humerus. IEEE Trans. Biomed. Eng. [Internet]. 2014;62(4):1–1. Available from: http://ieeexplore.ieee.org/lpdocs/epic03/wrapper.htm?arnumber=6949148doi:10.1109/TBME.2014.2368362

19. Myronenko A, Xubo Song. Point Set Registration: Coherent Point Drift. IEEE Trans. Pattern Anal. Mach. Intell. [Internet]. 2010 Dec;32(12):2262–2275. Available from: http://ieeexplore.ieee.org/document/5432191/doi:10.1109/TPAMI.2010.46

20. Nyffeler RW, Jost B, Pfirrmann CWA, Gerber C. Measurement of glenoid version: Conventional radiographs versus computed tomography scans. J. Shoulder Elb. Surg. 2003;12(5):493–496. doi:10.1016/S1058-2746(03)00181-2

21. de Oliveira ME, Netto LMG, Kistler M, Brandenberger D, Büchler P, Hasler C-C. An image-based method to automatically propagate bony landmarks: application to computational spine biomechanics. Comput. Methods Biomech. Biomed. Engin. [Internet]. 2015 Oct;18(14):1535–42. Available from: http://www.ncbi.nlm.nih.gov/pubmed/24960066doi:10.1080/10255842.2014.927445

22. Plessers K, Vanden Berghe P, Van Dijck C, Wirix-Speetjens R, Debeer P, Jonkers I, et al. Virtual reconstruction of glenoid bone defects using a statistical shape model. J. Shoulder Elb. Surg. [Internet]. 2017;1–7. Available from: https://doi.org/10.1016/j.jse.2017.07.026doi:10.1016/j.jse.2017.07.026

23. Poltaretskyi S, Chaoui J, Mayya M, Hamitouche C, Bercik MJ, Boileau P, et al. Prediction of the pre-morbid 3D anatomy of the proximal humerus based on statistical shape modelling. Bone Joint J. [Internet]. 2017 Jul;99–B(7):927–933. Available from: http://bjj.boneandjoint.org.uk.kuleuven.ezproxy.kuleuven.be/content/99-

B/7/927.longdoi:10.1302/0301-620X.99B7.BJJ-2017-0014

24. Rajamani KT, Styner M a, Talib H, Zheng G, Nolte LP, González Ballester M a. Statistical deformable bone models for robust 3D surface extrapolation from sparse data. Med. Image Anal. [Internet]. 2007 Apr [cited 2011 Jul 8];11(2):99–109. Available from: http://www.ncbi.nlm.nih.gov/pubmed/17349939doi:10.1016/j.media.2006.05.001

25. Scalise JJ, Codsi MJ, Bryan J, Iannotti JP. The three-dimensional glenoid vault model can estimate normal glenoid version in osteoarthritis. J. Shoulder Elb. Surg. 2008;17(3):487–491. doi:10.1016/j.jse.2007.09.006

26. Shi L, Griffith JF, Huang J, Wang D. Excellent side-to-side symmetry in glenoid size and shape. Skeletal Radiol. 2013;42(12):1711–1715. doi:10.1007/s00256-013-1728-y

27. Terrier a, Ston J, Larrea X, Farron a. Measurements of three-dimensional glenoid erosion when planning the prosthetic replacement of osteoarthritic shoulders. Bone Joint J. [Internet]. 2014 Apr [cited 2014 Oct 27];96–B(4):513–8. Available from: http://www.ncbi.nlm.nih.gov/pubmed/24692620doi:10.1302/0301-620X.96B4.32641

Tables & Figures

Table I – Effect of SSM-based prediction on OA glenoids. Predicted correction of glenoid version, inclination and medialization for the 30 scapulae with OA glenoids. The amount of correction was calculated separately for each Walch classification. Results are reported as mean ± standard deviation where applicable. Positive (negative) signs corresponds to increase (decrease) of the respective measure in the present OA shape relative to the SSM-based reconstructed premorbid shape. For example, a negative change in version means that the SSM-based prediction corrects the posterior OA wear to a more neutral orientation.

	N	Δ version (°)	Δ inclination (°)	Δ medialization (mm)
A1	7	1.4±2.9	2.9±5.0	-0.2±1.3
A2	5	-6.3±8.5	2.8±4.1	0.6±1.4
B1	5	0.7±1.8	1.0±2.6	0.1±0.7
B2	11	-8.1±4.6	1.0±4.5	-0.8±0.9
B3	1	-22.6	4.5	0.3
D	1	8.9	-3.9	1.0

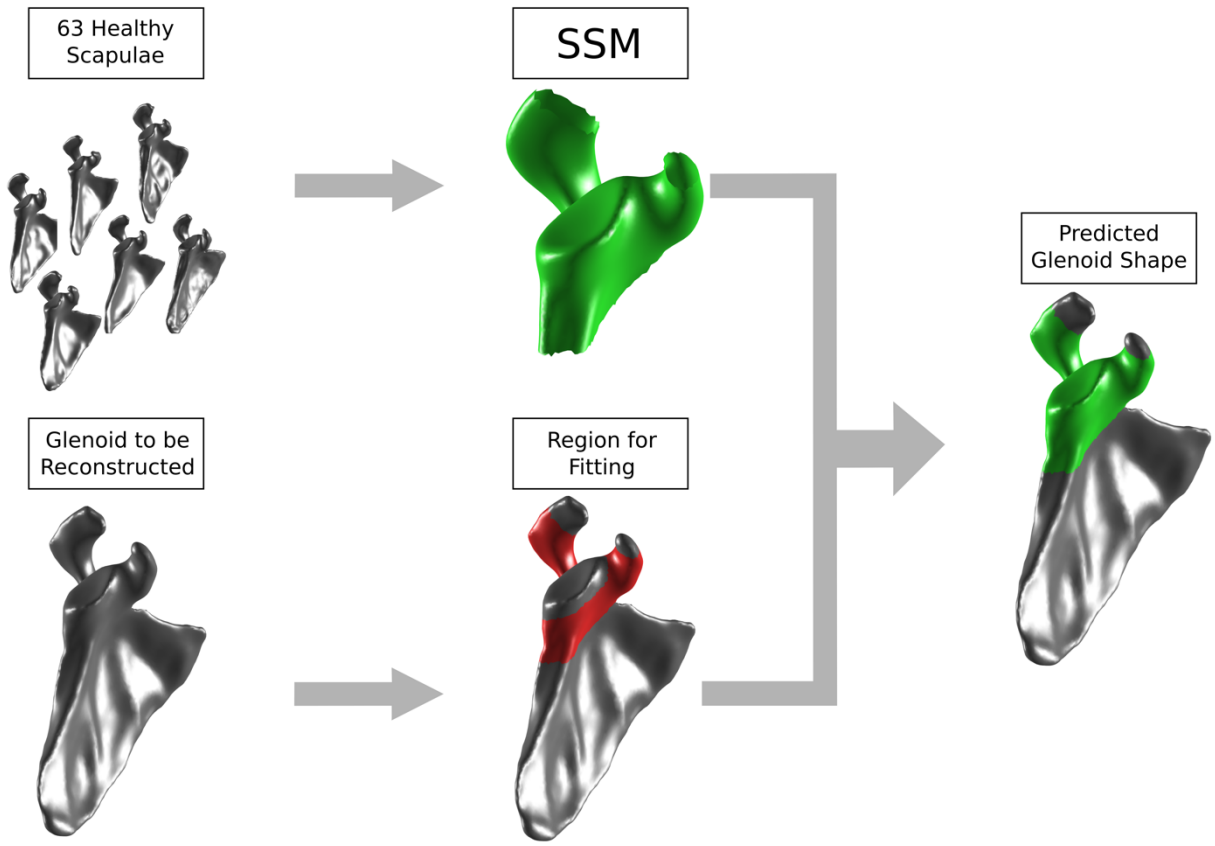

384

385 **Figure 1 – SSM-based prediction of premorbid glenoid surface:** A SSM was built from a
386 population of healthy glenoid surface models. The predicted premorbid glenoid cavity of a specific
387 scapula was obtained by fitting the SSM to the bony region surrounding the glenoid cavity (red
388 area). Based on local fitting, the SSM provided the shape of the healthy glenoid (green area). The
389 performance of the prediction approach was evaluated on healthy scapulae following a leave-one-
390 out strategy.

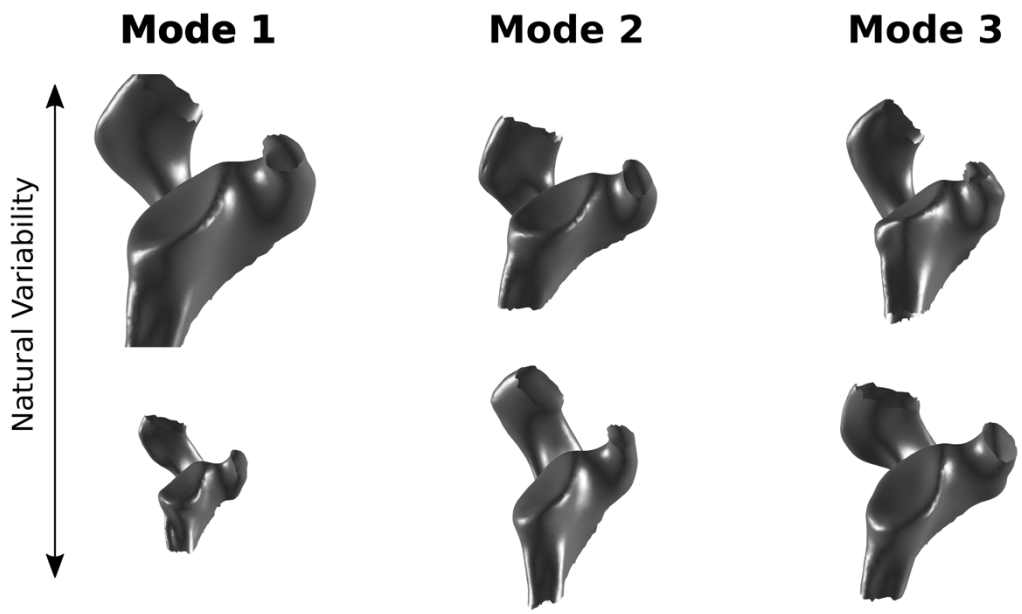

391

392 **Figure 2 – Statistical shape model of healthy scapulae:** The three major modes of variation of
393 the SSM constructed from all the training data are represented. These modes account for
394 approximately 40%, 13%, and 9% of the overall variability across subjects, respectively.

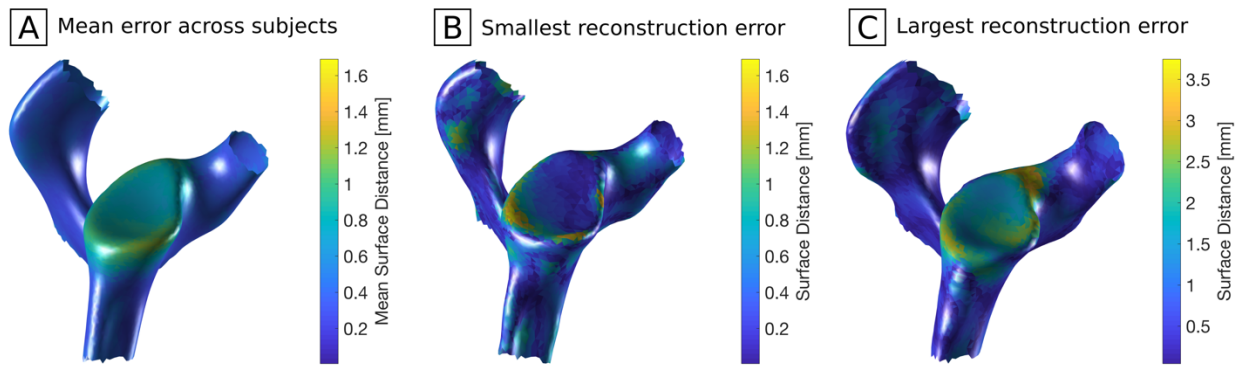

Figure 3 – Surface reconstruction error on healthy scapulae: Pointwise average surface distances between original and reconstructed shapes of the glenoid region. The extent of the surface model was chosen to minimize glenoid reconstruction error. Figure (A) shows the average surface distance across subjects on the mean shape of the healthy scapulae dataset. Figures (B) and (C) show shape and surface distance for the best and worst fitting scapula, respectively.

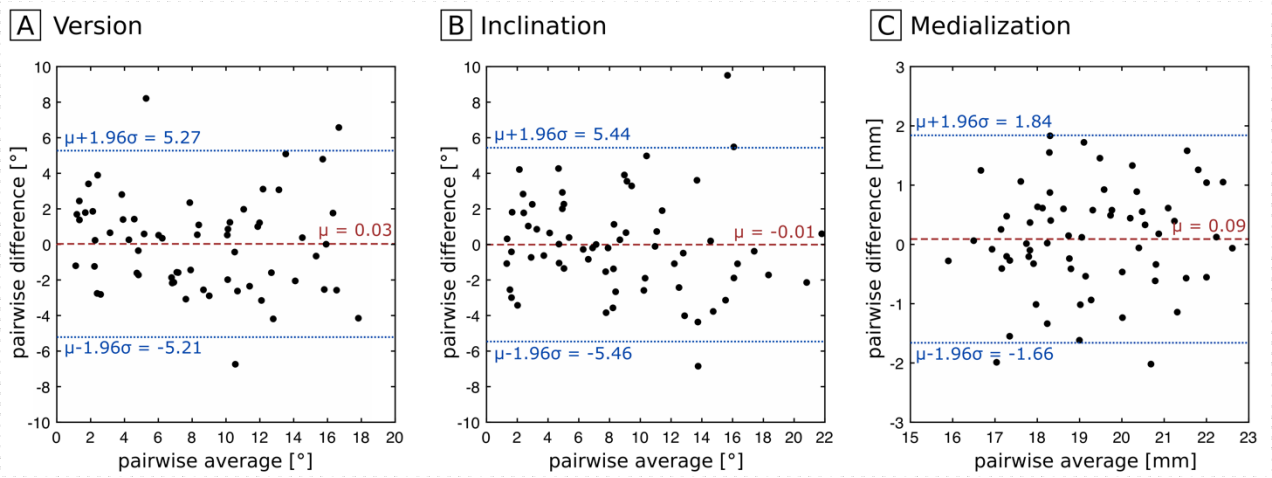

401

402 **Figure 4 – Glenoid reconstruction error on healthy scapulae: Bland-Altman representations**
403 **of differences between original and reconstructed glenoid characteristics.** Subfigures (A), (B),
404 and (C) show the reconstruction errors between original and predicted glenoid version, inclination,
405 and medialization. The x-axis (y-axis) refers to the average (difference) between original and
406 predicted value of each measurement. Mean and 95% limits of agreement of the differences
407 between original and predicted measurements are indicated by dashed red and dotted blue lines,
408 respectively.

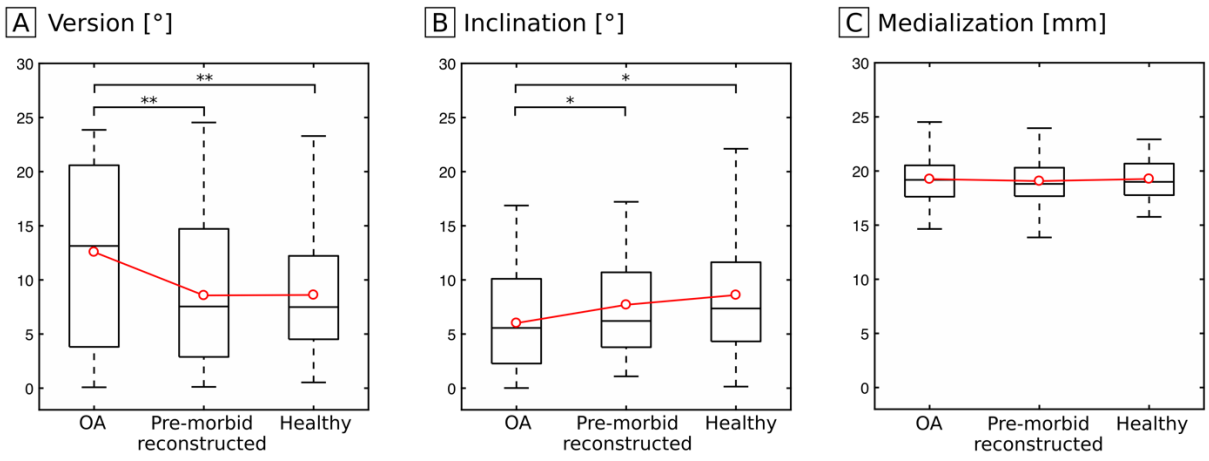

Figure 5 – Comparison of glenoid version, inclination and medialization between OA glenoids, the SSM-based reconstructions and the healthy population. Statistically significant differences between groups are indicated by star markers, where ** corresponds to $p < 0.01$, * to $p<0.05$ and no marker to $p>0.05$. Comparisons between groups 'OA' and 'pre-morbid reconstructed' are based on paired Student's t-test; comparisons with 'healthy' on unpaied two sample Student's t test. The red markers indicate the mean of each group.